Characterization of Niti Super Elasticity Shape Memory Alloys

Dr. Sahib M. Al-Saffar
Materials Engineering Department, University of Technology/Baghdad
Dr. Emad S. Al-Hassani
Materials Engineering Department, University of Technology/Baghdad
Rasha Ali Hussein
Materials Engineering Department, University of Technology/Baghdad
Email:eng_rahmas@yahoo.com

Received on: 16/10/2011 & Accepted on: 11/6/2013

ABSTRACT

Ni-Ti samples were prepared by powder metallurgy. The prepared samples were master samples M_1 (55% Ni- 45%Ti) and M_2 (56% Ni- 44%Ti). The additive percentage of Ta was 5%, 7% and 9% to master sample M_1 and M_2, while Nb addition was 1%, 2% and 4% to M_1 and M_2. The pressure of pressing was 800 Mpa. The samples were sintered at 950 °C for a time of 9 hr. Samples were then examined by using SEM technique, XRD, DSC, Vickers hardness. The porosity was measured according to Archimedes method.

Scanning electronic microscopy images showed that most prepared samples have porosity, which in turn imparts decreasing microhardness values across the surface. Better increase of microhardness values is found in M_2+5%Ta. Scanning electron microscopy indicated also the best martensitic structure in M_1+4% Nb and M_2+4%Nb. X-ray diffraction observations indicated that NiTi, Ni_3Ti and $NiTi_2$ phases exist in all samples. NiTi phase is playing a dramatic role in enhancing shape memory effect and superelasticity. DSC results show that transformation temperatures range in (46-134°C). This indicates that all samples at room temperature have one phase which is martensite.

توصيف سبائك ذاكرة الشكل NiTi فائقة المرونة

الخلاصة

استخدمت تكنولوجيا المساحيق كطريقة اساسية لتحضير العينات الخاصة بالبحث وكانت درجة حرارة التلبيد المستخدمة هي ٩٥٠ °م ولزمن إبقاء ٩ ساعات. تم تحضير العينات بشكل مجاميع حسب مكوناتها حيث حضرت عينيتين رئيسيتين (بدون إضافات) وهي M_1 والتي تحتوي على (٥٥ % نيكل +٤٥ % تيتانيوم) وM_2 التي تحتوي على (٥٦ % نيكل +٤٤% تيتانيوم). تم اضافة عنصر التنتالوم بنسب (٥% و ٧% و٩%) أضيفت للعينات الرئيسية M_1 و M_2 ، اما النيوبيوم

https://doi.org/10.30684/etj.31.16A.3
2412-0758/University of Technology-Iraq, Baghdad, Iraq

فكانت إضافته بنسب (١% و ٢% و ٤%) للعينات الرئيسية M_1 و M_2 . ان الضغط المستخدم في عملية الكبس هو (٨٠٠ Mpa).

بعد عملية تحضير العينات تم أجراء الفحوصات التالية: تحليل المجهر الالكتروني الماسح، وتحليل حيود الاشعه السينية، ومقياس الحرارة الماسح التفاضلي، والصلادة بطريقة فيكرز والمسامية بطريقة ارخميدس.

وباستخدام تحليل المجهر الالكتروني الماسح فأن اغلب العينات المحضرة تحتوي على مسامية واضحة، والتي بدورها تؤدي إلى تقليل قيم الصلادة المايكروية على السطح. إن أفضل زيادة في قيم الصلادة المايكروية وجدت في العينة T_2 (M_2+ 5% Ta)، و من نتائج المجهر الالكتروني الماسح فأن أفضل تركيب نسيجي مارتنسايتي كان في العينتين N_5 *(M_1+4% Nb)* و *(M_2+4%Nb)* . N_6 وبين تحليل حيود الاشعه السينية إلى أن الأطوار NiTi و Ni_3Ti و $NiTi_2$ موجودة في جميع العينات، ان طور NiTi يلعب دور رئيسي في تعزيز تأثير ذاكرة الشكل والمرونة الفائقة. أن نتائج مقياس الحرارة الماسح التفاضلي تظهر ان درجات حرارة التحول للعينات تتدرج بين (٤٦-١٣٤ °م)، وهذا يعني بأن جميع العينات في درجة حرارة الغرفة تحتوي على طور واحد وهو المارتنسايت. أما نتائج اختبار الصلادة المايكروية وفحص المسامية فأنها تبين بأن M_2 لها أكثر صلادة وأقل مسامية من M_2 ، وأن إضافة كل من التنتالوم والنيوبيوم غالبا ما تؤدي إلى زيادة بالمسامية وتقليل بالصلادة.

INTRODUCTION

Shape memory alloys (SMA) are materials that have the ability to return to a former shape when subjected to an appropriate thermo mechanical procedure. Pseudoelastic and shape memory effects are some of the behaviors presented by these alloys. The unique properties concerning these alloys have encouraged many investigators to look for applications of SMA in different fields of human knowledge [1].

Shape memory alloys (SMAs) are deformed at a low temperature, some residual strain remains after unloading. However, the residual strain vanishes and SMAs return to its original shape by a reversible transformation upon heating. The property is related to the reversible martensitic phase transformations, which are solid-solid diffusionless processes between a crystallographically ordered phase (austenite) and a less ordered phase (martensite) [2].

NiTi alloys are the most promising Shape Memory Alloys in terms of practical applicability; due to their special functional properties, namely one way or two way shape memory effect (OWSME, TWSME) and superelastic effect (SE). NiTi components have seen growing use in recent years in a number of industrial fields as biomedical, automotive, and aeronautic and many others [3].

The Ni-Ti alloys have been successfully applied as biomaterials such as orthodontics arch wires, guide wires and stents in addition to many engineering applications. The Ni-Ti alloys are also considered as one of the attractive candidates for orthopedic implants [4]. There is a new class of SMAs known as *High Temperature Shape Memory Alloys* (HTSMAs). HTSMAs are a unique class of SMAs that have transformation temperatures greater than 100 ºC and are capable of actuating under high temperature conditions. These alloys are produced by adding ternary elements such as palladium, platinum, hafnium, gold, and zirconium to NiTi, for which the transformation temperatures can be shifted anywhere in the range of (100-800) ºC [5,6,7].

The aim of this study is to prepare NiTi alloys as master alloy and then study the effect of different additives of Ta and Nb individually, on the characteristics of NiTi.

The purpose of experimenting the physical characteristics and transformation temperatures of alloys is to candidate the better percentage of additives for different applications.

EXPERIMENTAL WORK

Samples Preparation

NiTi samples were prepared using powder metallurgy, which consists of mixing, compacting and sintering processes. The powders were taken from different chemical companies. The purity, the average particle size and origins of the powders used in this work are shown in Table (1). Ni-Ti powder (master mixture; 55 wt% Ni with 45 wt% Ti and 56 wt% Ni with 44 wt% Ti) was prepared using a ball mill mixer for two hours. This mixture was used to prepare three groups as shown in Table (2); first master alloy in two samples (without additives). Other samples were prepared with 5, 7 and 9 wt% of Ta and with 1, 2 and 4 wt% of Nb additions by mixing in the ball mill for two hours for each percentage.

Pressing

After mixing, a 5 gm of each sample were compacted at 800 MPa. Pressing was done by a hydraulic pressing machine in a tool steel die (15 mm) in a diameter.

Sintering

Each sample was sintered in a vacuum furnace at a temperature (950) ºC for (9) hours with a heating rate of (10) ºC/min.

X-Ray Diffraction Test

X-ray diffraction test was done to identify the formed phases of sintered samples. By using XRD instrument type D8 II machine, Bruker axs, 240V, 50Hz and 6.5 KVA made in Germany

Microstructure Observation (SEM)

Surface microstructure was observed by using Scanning Electron Microscopy (SEM) for each sample after sintering using SEM type (TM-1000 Hitachi Tabletop, Japan).

Microhardness Measurements

Vickers microhardness method was used to measure the hardness of the sintered samples at loading of (1.0 Kg) held for 10 seconds. The values of hardness have been taken from five different places along the surface for each sample and the averages of 5 readings have been taken to get the hardness value. This test is achieved by using vickers hardness testing machine type (Fv 800 Future-Tech Tester, Japan).

Porosity

Porosity was measured by using Archimedes method (depending on weighting of sintered samples) as follows:[8]

$$Porosity\ (\%) = \frac{W_s - W_d}{W_s - W_n} * 100\ \% \qquad \ldots (1)$$

Where:

W_s = weight of sample after immersing in distilled water for 24 hours.

W_d = weight of the dry sample after sintering.

W_n = weight of immersed sample in distilled water and suspended in air.

Transformation Temperatures

The transformation temperatures were measured for each sample using the DSC (Differential Scanning Calorimeter) type Mettler Toledo, Switzerland, by taking (5-10) mg of each sample and testing at a scan rate of 15 ºC/min. The cooling agent used in the DSC (in order to cool up to -50 °C) was liquid Nitrogen. While maximum temperature was 200 °C.

RESULTS AND DISCUSSION

Chemical Compositions

All prepared samples were examined using energy dispersive spectrum (EDS) for the chemical composition analysis. The structure was obtained after etching with an etching solution (10 ml of HF, 20 ml of HNO_3 and 150 ml of H_2O distilled water) at room temperature [9].

Figures (1 and 2) show the EDS spectrum and chemical composition of the master samples M_1 (55 % Ni + 45 % Ti) and M_2 (56 % Ni + 44 % Ti), respectively. Tables (3 and 4) show the chemical composition of master samples (M_1 and M_2 respectively). Figures (3 and 4) show the EDS spectrum and chemical composition of the master samples with Ta additives. Figures (5 and 6) show the EDS spectrum and chemical composition of the master samples with Nb additives.

The samples (M_1, M_2, T_5, T_6, N_5 and N_6) were investigated using EDS spectrum in order to find their chemical compositions. Samples were prepared to have 45 wt % Ti (i.e. 55 wt % Ni) for the master sample (M_1) which corresponds to 44.37 wt % Ti and 48.45 wt % Ni in EDS results. The other master sample (M_2) has 44 wt % Ti (56 wt % Ni) which corresponds to 43.13 wt% Ti and 49.49 wt % Ni. On the other hand the prepared samples with additives (Ta and Nb) which have the higher values of additions as shown in figures (3, 4, 5 and 6). Since the percentages of additions Ta and Nb are small percentages to cause significant change in composition, so the maximum percentages of addition of Ta and Nb which are 9 wt% and 4 wt %, respectively, had been taken to EDS analysis.

Scanning electron microscope images of all etched samples are shown in figures (7 to 20). The martensite formed in all alloys has needle shaped grains, because of diffusionless feature of martensitic transformation; the ordered or disordered of the parent phase (B_2) is transformed to martensite. Disordered B_2 forms disordered martensite B19′ [10]. All investigated phases appear in the form of dark and grey spots and small white dots immersed in the matrix. Some of the phases accumulate at the grain boundaries because of the high free energy of the grain boundaries. Figures (18, 19 and 20) show the needle shaped microstructure of martensite which appeared in ordered pattern. These figures are smilar to samples with Nb addition.

XRD Patterns

The sintered samples were examined with X-rays. Figures (21-22) show the diffraction patterns for the master samples no pure metals was observe which indicate that the sintering time and temperature used in this work result in complete sintering reaction. Figures (21- 22) show that the samples compacted at 800 MPa consist mainly of two phases; the martensitic phase (monocline) and the austenitic phase (cubic), in addition to Ti_2Ni, Ni_3Ti, Ni_4Ti_3 and Ni_2Ti. The formation of Ti_2Ni and Ni_3Ti might be attributed to the slow cooling of the samples with the furnace cooling rate whereas, in the sintering condition used throughout this work, the free Gibbs energies for Ni_3Ti and Ti_2Ni were less than that for NiTi and it seems difficult to

obtain a final equilibrium structure of NiTi alone just by solid –state diffusion [11]. No pure Ni was found in NiTi alloys after sintering at 950 °C and time 9 hr, in which B2 (NiTi) is the dominant phase. The sintering is complete as NiTi, Ti_2Ni and Ni_3Ti are stable phases. The NiTi phase is obviously dominant while Ni_3Ti and Ti_2Ni are not. This can be attributed to the high sintering temperature, which enhances the diffusion rate and makes the reaction tend to equilibrium [12]. The addition of Ta to the NiTi binary alloy can improve its X-ray visibility [13].

Transformation Temperatures

The transformation temperatures, which are used to determine the temperatures at which the austenitic and martensitic phases may exist, were characterized by DSC at a scan rate of 15 °C/min for all prepared samples. Figure (23) show the transformation temperatures for the master samples (M_1 and M_2). It is seen that the master samples have 58 °C as M_f (martensitic finish temperature) for M_1 and M_2, and (134 °C and 130 °C) as A_f (austenitic finish temperature) for M_1 and M_2 respectively. This means that both the master samples at room temperature consist of martensite. From that it is seen that a small difference in the chemical composition does not influence in the transformation temperature.

The equiatomic composition (i.e. 50 at% of Ni and Ti) exhibits the maximum A_f temperature (120 °C) of all NiTi compositions studied. Decreasing the Ni atomic percentage (at. %) from the equiatomic composition does not change the transformation temperatures. If the composition of nickel is increased above 50 at.% , the transformation temperature begins to decrease, with A_f becoming as low as - (40) °C for 51 at.% nicke [14]. Figure (23) shows that the increase in the percentage of Nickel of 1 wt % will decreased A_f about 4°C. The addition of Ta led to a significantly raising As(*austenitic start temperature*) and Ms*(martensitic start temperature*) increased but slightly. When Ta content is in a range from 5 at.% to 35 at.%, all of the transformation temperatures just increased slightly. Since it is well known that in NiTi binary alloys, the phase transformation temperature decreases with increasing the Ni/Ti ratio [13]. The addition of Nb increased slightly the values of A_s and M_s by increasing Nb percentage as shown in figure (23). The values of M_f were not affected by any addition and ranged between (46 °C - 60.5 °C).

Vickers Hardness

The hardness measurements are shown in Figures (24-25). Hardness measurements were made for master samples (M_1 and M_2) and these values will be compared to those of the prepared samples with additives (Ta and Nb). Figure (24) shows that measurement hardness value of M_2 is higher than that for M_1. This difference can be attributed to the fact that the sample M_1 has more porosity than the sample M_2 as shown in Figure (25). SEM images for M_1 and M_2 samples Figures (7 and 8) show more pores and even larger sized pores in M_1 than that in M_2. It is known that the martensite is softer and more ductile than austenite, i.e. the latter is stronger and hard in this system [15, 16]. In comparison with the master samples values of hardness, one can find that the hardness decreases with increasing Ta as shown in Figure (24). It is clear that sample T_2 has the higher value of hardness which is 331 (Hv), Figure (25) shows that the measured hardness decreases by increasing Nb addition. The sample of 1% wt Nb addition has higher hardness than the hardness of the masters M_1 and M_2. This drop in hardness may attribute to some phases and pores localized on the surface [17], have shown that the alloy primarily consists of the NiTi

phase with dispersed insoluble elliptical or globular precipitates of nearly pure Nb. These precipitates are extremely soft [14].

Porosity

The porosity percentages of the prepared samples are extracted by Archimedes method. Figure (26) shows that the porosity percentage for the master sample (M_1) is higher than that for (M_2) because of the most powder used for compaction have irregular shape. The addition of fine spherical powder Ni effectively decreases porosity percentage in M_2. SEM of Figure (7 and 8) shows M_1 is higher porosity than M_2. Figure (26) shows the porosity increased with increasing Ta addition; because of less adhesion and interdiffusion between the particles. Figure (27) shows that the porosity percentage increases with increasing the percentage of Nb wt% which could be attributed to particles to be sintered are smaller than 1 mm in size and can possess a wide variety of geometries: spheres, cubes, wires, flakes, discs, snowflakes, or other small solids that flow and pack as a powder [18], that may enhance forming small pores thus increasing the porosity. Figures (15 - 20) show how the porosity increases gradually with increasing Nb wt%.

CONCLUSIONS

1. The addition of 1wt % Nb may result in increase in hardness. But for more than 1% Nb that will decrease the H_v.
2. Small amount of Ta addition, it can improve the hardness but this can be the opposite if Ta addition increased.
3. Ta and Nb addition results in increasing in porosity compared with master samples (without additives).
4. X-ray diffraction technique showed that sintering at 950 °C for 9hr is efficient to satisfy sintering process in which elemental powders are completely transformed into alloy structure.
5. Phase transformations occurred in a temperature range of (46-134 °C) as indicated by DSC. All samples have one phase at room temperature which it is martensite.

REFERENCES

[1].Machado L.G. And Savi M.A., "Medical applications of shape memory alloys", Brazilian Journal of Medical and Biological Research, 36:683-691, (2003).

[2].Daqiang Jiang, Lishan Cui, Yanjun Zheng and Xiaohua jiang, "Effects of thermal cycling on the temperature memory effect of TiNiNb Alloy", Journal of materials engineering and performance, vol.19, no.7, pp. 1022-1024 October, (2010).

[3].Andrea Falvo, "Thermo-mechanical characterization of Nickel-Titanium shape memory alloys", Ph.D. thesis, department of mechanical engineering, university of Della Calabria, Italia, 2008.

[4].Takayuki Yoneyama and Shuichi Miyazaki, "Shape memory alloys for biomedical applications", Woodhead publishing in materials .Ltd., Cambridge, England, pp. 3, 4, 114, 258, 281, (2009).

[5].H.Funakubo (Ed.), "Shape memory alloys", Gordon and Breach scientific publishers, pp. 239-245 (1987).

[6].P.G.Lidquist and C.M.Wayman, "Shape memory and transformation behavior of martensitic Ti-Pd-Ni and Ti-Pt-Ni alloys", in: T.W. Duerig , K.N. Melton , D.Stöckel , C.M. Wayman (Eds.), Engineering Aspects of Shape Memory Alloys, Butterworth- Heinemann, London, pp.(58-68), (1990) .

[7].P.E. Thoma, J.J. Boehm, "Effect of composition on the amount of second phase and transformation temperatures of Nix Ti90 - x Hf shape memory Alloys" Materials science and Engineering A273-275, pp.(385-389), (1999).

[8].ASTM, "Annual Book of ASTM Standards", Section (10); Electrical Insulation and electrons Volume (15.05), USA,(1988).

[9].L.M. Gammon, R.D. Briggs, J.M. Packard, K.W. Batson, R. Boyer, C.W. Domby, Metallography and Microstructures of Titanium and Its Alloys, *Metallography and Microstructures,* Vol 9, *ASM Handbook*, ASM International, pp. 899–917, 2004.

[10].Emad Saadi AL-Hassani, "Preparation and Corrosion Behavior of NiTi Shape Memory Alloys" Ph.D. Thesis, University of Technology, Iraq, (2007).

[11].Li Bing-yun, Li-Jian, Yi-Yi, "Porous NiTi Alloy prepared from Elemental Powder Sintering", Chinese Academy of Science, Vol.13, No.10, pp.(2847-2851), January, (1998).

[12].Hey J.C.,and Jordine A.P.," Shape memory TiNi synthesis from elemented powders ", Material Science and Engineering, A 188, pp. 291-300,(1994).

[13].Jianlo MA, Jiangnan LIU , Zehngpin WANG ,Fei Xue , Kuang-His WU , and Zhongjie PU, " Effects of Ta Addition on NiTi shape Memory Alloys", Journal of Material Science Technology, volume 16, no. 5, pp(534-536) , (2000) .

[14].Dimitrisn C.Lagoudas, "Shape Memory Alloys-Modelling and Engineering Application", Springer Science + Business Media LLC, Department of Aerospace Engineering, Texas A&M University, College Station, USA, pp. (2-6, 23-41,281), (2008).

[15].K.Shimzu, and Tadaki T. , " Shape Memory Effect Mechanism " Gordon and Breach Science ,New York , pp.(1-60) , (1978).

[16].S.Miya zaki ,A.Ishida" Martensitic Transformation and shape Memory behavior in Sputter –Deposited NiTi Base Thin Films", Materials Science and Engineering ,A 273-275,pp.(112-126) , (1999).

[17].L.C.Zhao ,T .W. Duerig, S.Justi,K.N.Melton , J.L.Proft, W.Yu, C.M.Wayman, " the study of Niobium-rich precipitates in a Ni-Ti-Nb shape memry alloy scripta Metallurgica and Materialia Vol.24 ,pp(221-226) , (1990).

[18].Mark A.Whitney, "A study of the Sintering Behaviour of Ni-Ti powder compacts using Differential scanning Calorimetry", MS.C.Thesis, the University of Waterloo Ontario, Canada, (2007).

Table (1) Powder metals used.

Metal (Powder)	Purity (%)	Average of Particle Size (μm)	Manufacturing Company
Ni	99.7	3	METCO, ENGLAND
Ti	99.5	150	FLUKA-, SWISS
Ta	99.98	45	STREM CHEMICALS, USA
Nb	99.8	45	STREM CHEMICALS, USA

Table (2) Descriptions of prepared samples.

Alloys	Samples No.	Samples Code	Descriptions (Wt %)
Master alloys	1	M_1	55 % Ni + 45 % Ti
	2	M_2	56 % Ni + 44 % Ti
Ni + Ti + Ta	3	T_1	M_1 + 5 % Ta
	4	T_2	M_2 + 5 % Ta
	5	T_3	M_1 + 7 % Ta
	6	T_4	M_2 + 7 % Ta
	7	T_5	M_1 + 9 % Ta
	8	T_6	M_2 + 9 % Ta
Ni + Ti + Nb	9	N_1	M_1 + 1 % Nb
	10	N_2	M_2 + 1 % Nb
	11	N_3	M_1 + 2 % Nb
	12	N_4	M_2 + 2 % Nb
	13	N_5	M_1 + 4 % Nb
	14	N_6	M_2 + 4 % Nb

Table (3) ED's analysis for master sample (M1).

Elements	Atomic Number	Series	Wt. % (Total 100.00)	At. % (Total 100.00)	Error [%]
Nickel	28	K-series	48.45	38.84	2.1
Titanium	22	K-series	44.37	43.60	1.8
Oxygen	8	K-series	3.32	9.75	7.4
Aluminium	13	K-series	2.39	4.17	0.3
Fluorine	9	K-series	1.47	3.64	0.6

Table (4) ED's analysis for master sample (M_2).

Elements	Atomic Number	Series	Wt. % (Total 100.00)	At. % (Total 100.00)	Error [%]
Nickel	28	K-series	49.49	38.58	1.9
Titanium	22	K-series	43.13	41.22	1.6
Oxygen	8	K-series	2.84	8.12	5.7
Nitrogen	7	K-series	2.18	7.13	4.4

Fluorine	9	K-series	1.34	3.22	0.4
Aluminium	13	K-series	1.02	1.73	0.1

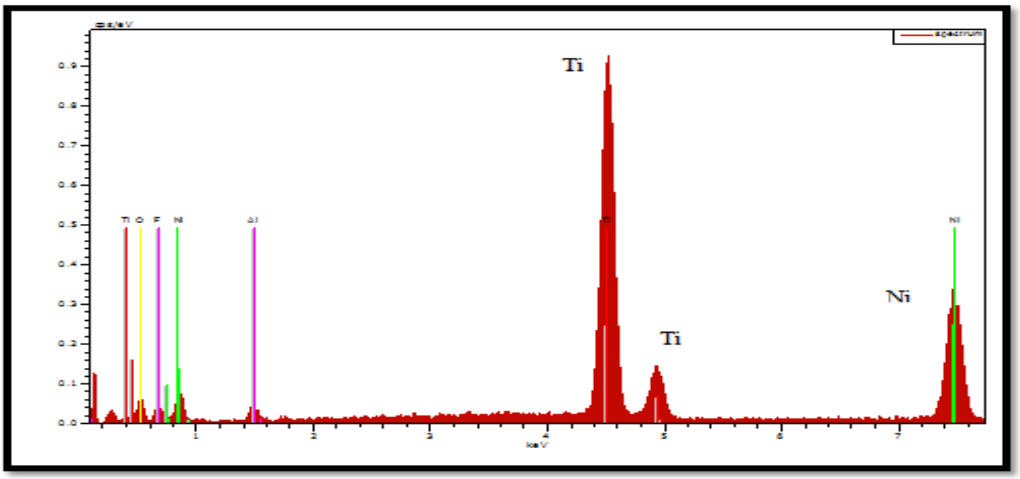

Figure (1) ED's spectrum for master sample (M1).

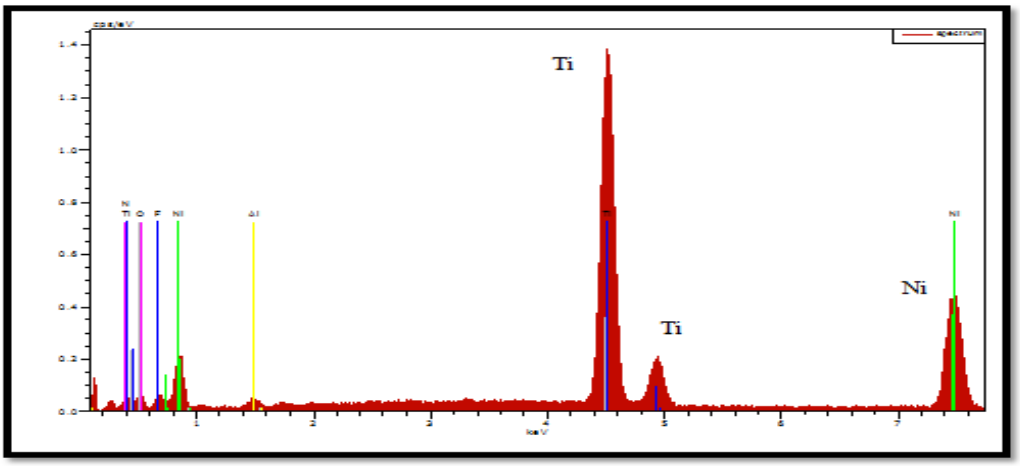

Figure (2) ED's spectrum for master sample (M2).

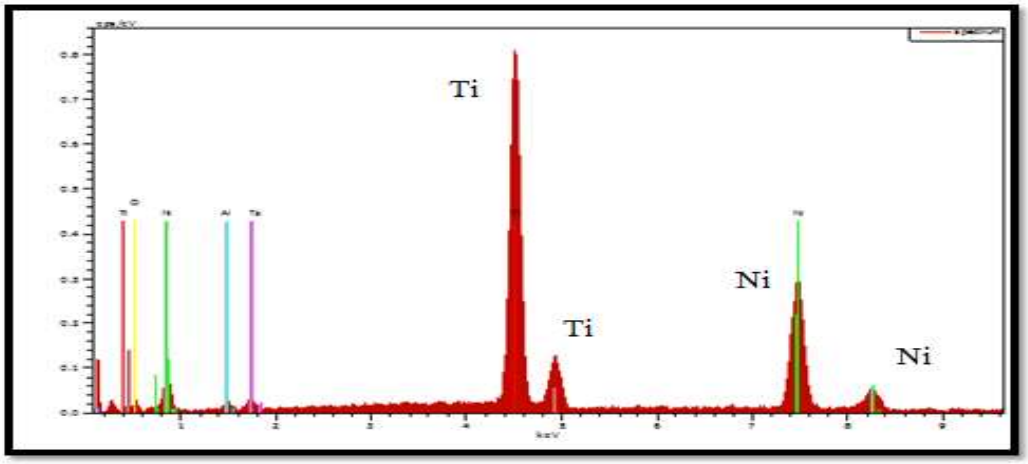

Figure (3) ED's spectrum for (T5) sample.

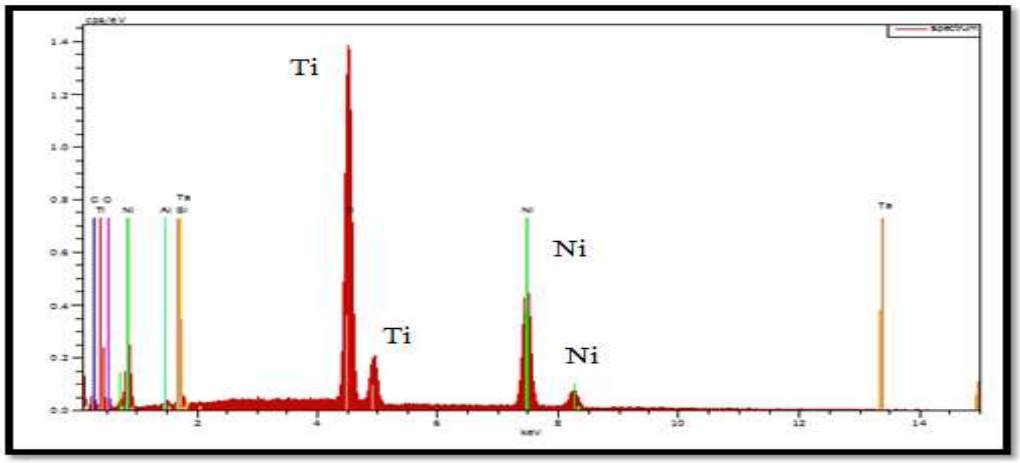

Figure (4) ED's spectrum for (T6) sample.

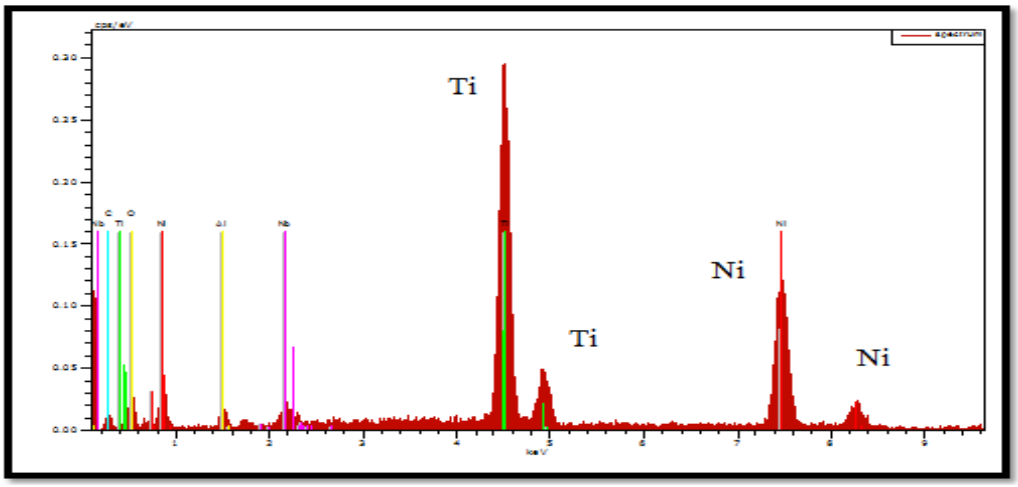

Figure (5) ED's spectrum for (N5) sample.

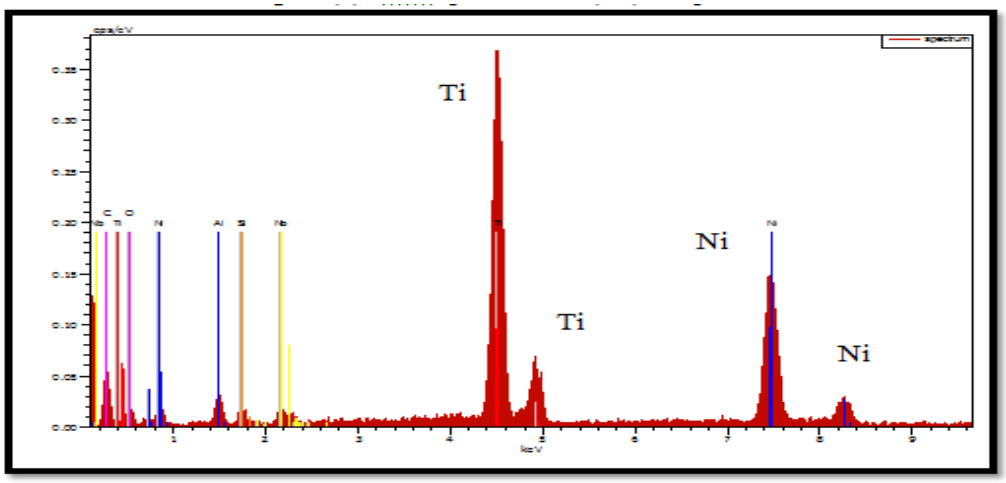

Figure (6) ED's spectrum for (N6) sample.

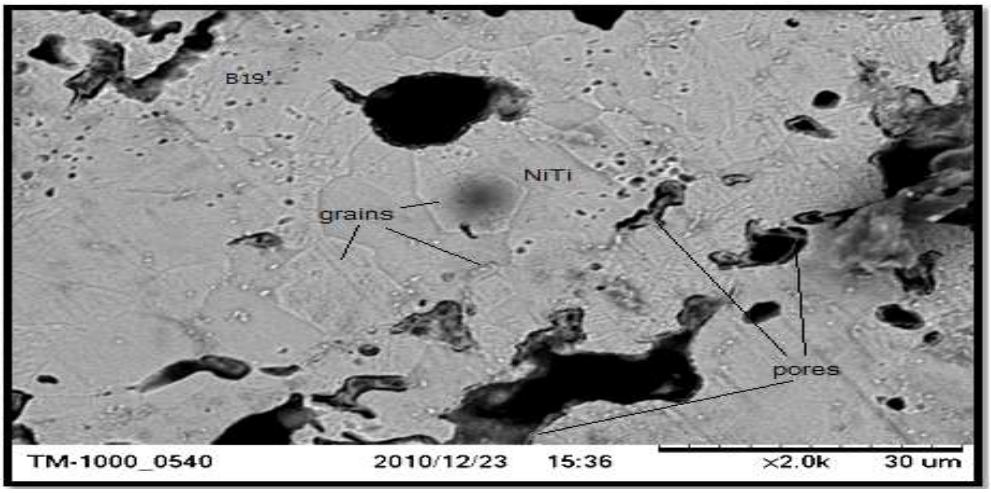

Figure (7) SEM micrograph of etched sample (M_1).

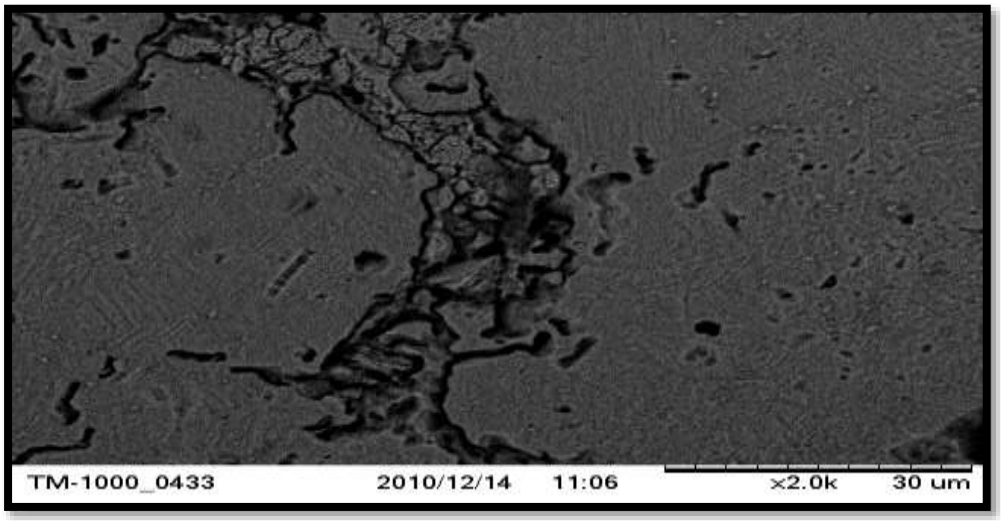

Figure (8) SEM micrograph of etched sample (M2).

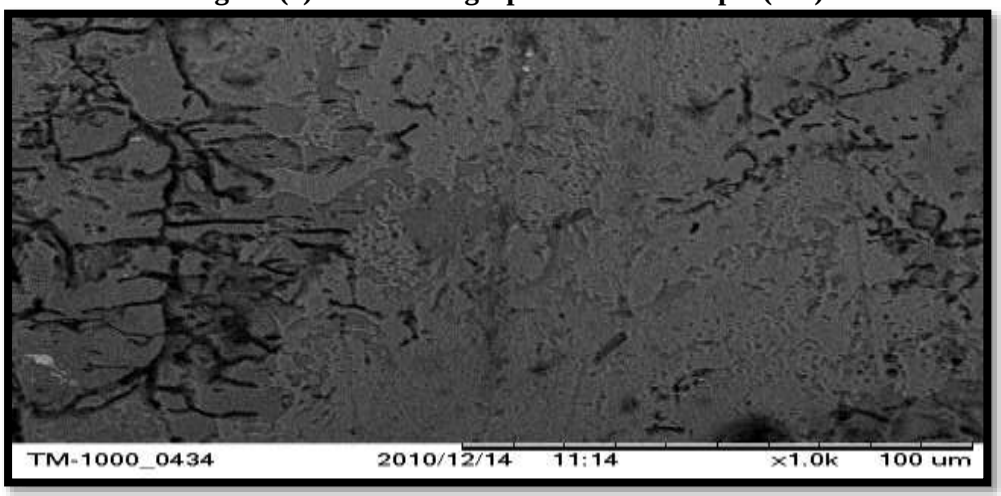

Figure (9) SEM micrograph of etched sample (T1).

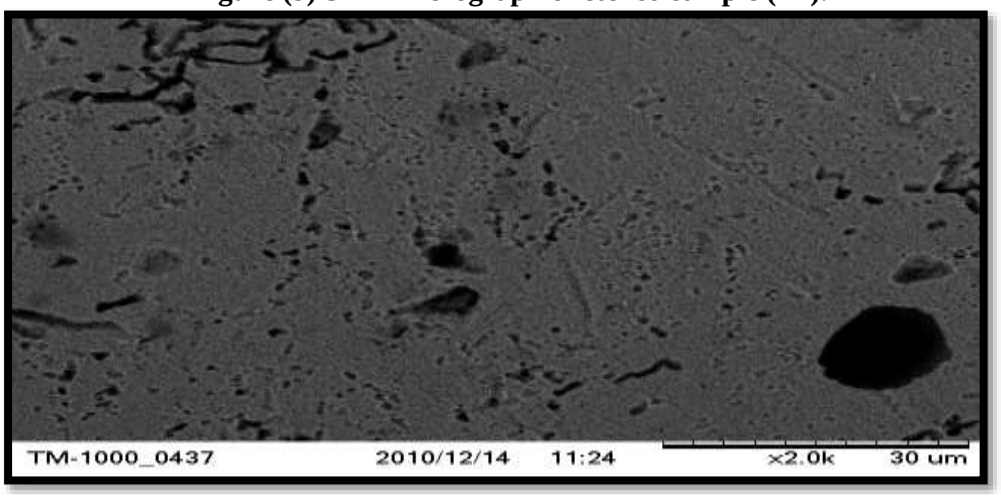

Figure (10) SEM micrograph of etched sample (T2).

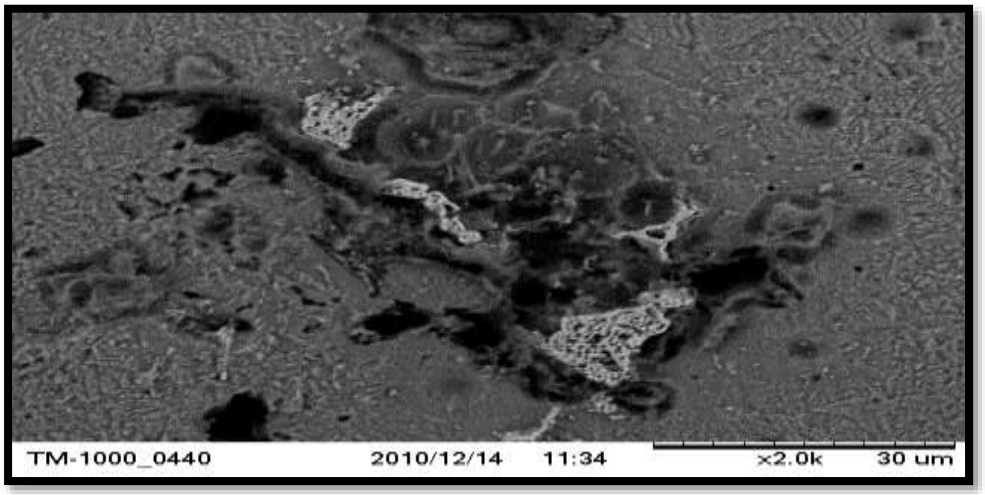

Figure (11) SEM micrograph of sample (T3).

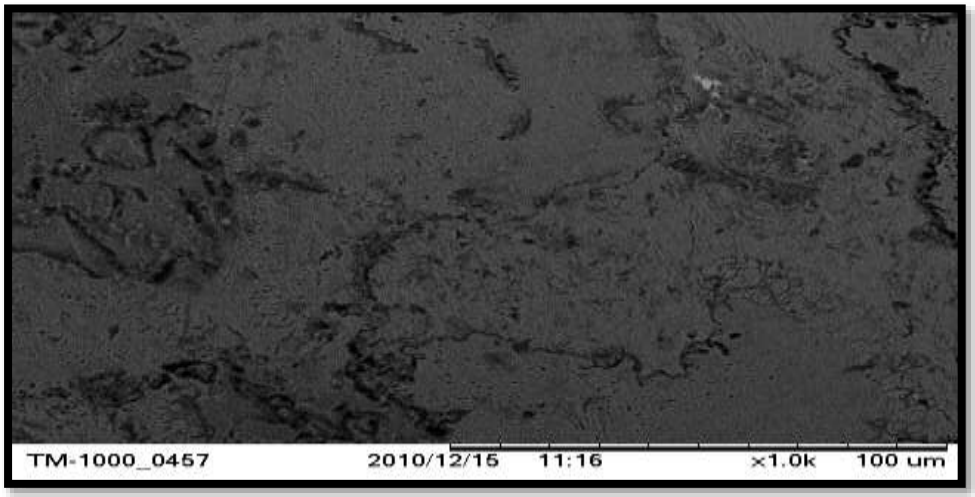

Figure (12) SEM micrograph of sample (T4).

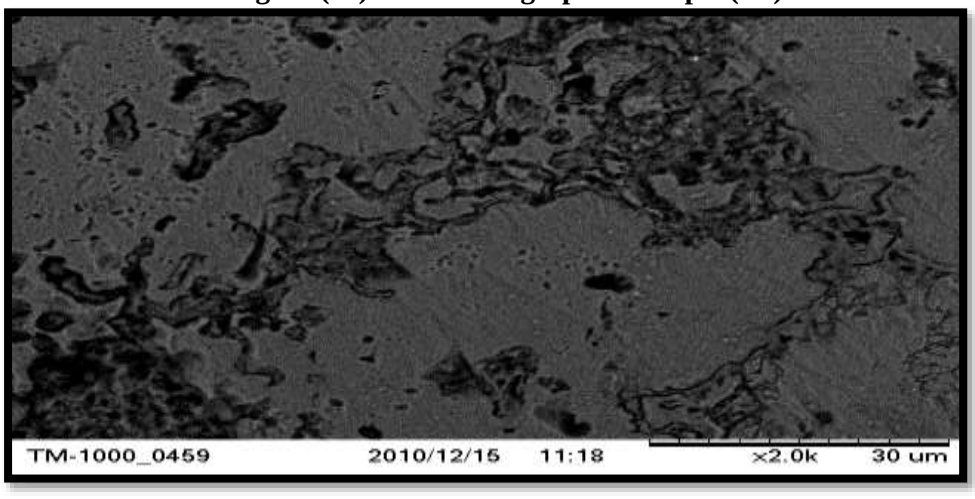

Figure (13) SEM micrograph of sample (T5).

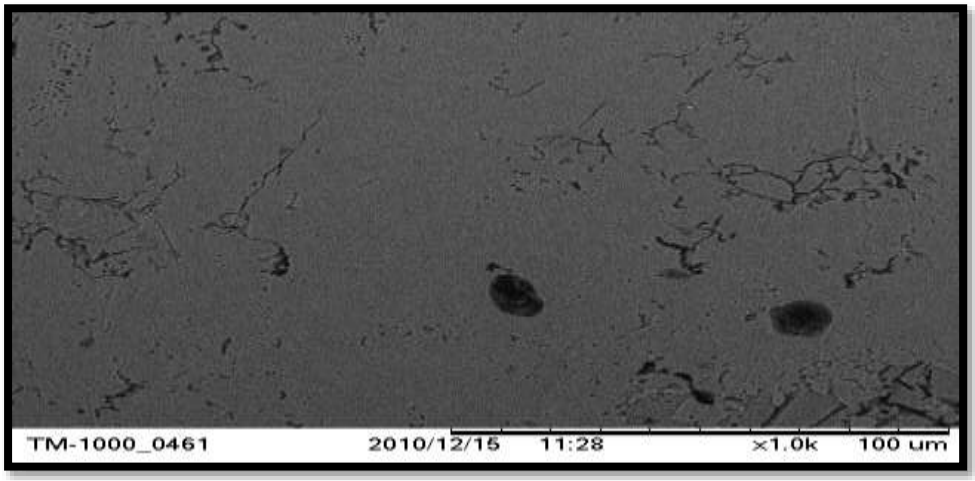

Figure (14) SEM micrograph of sample (T6).

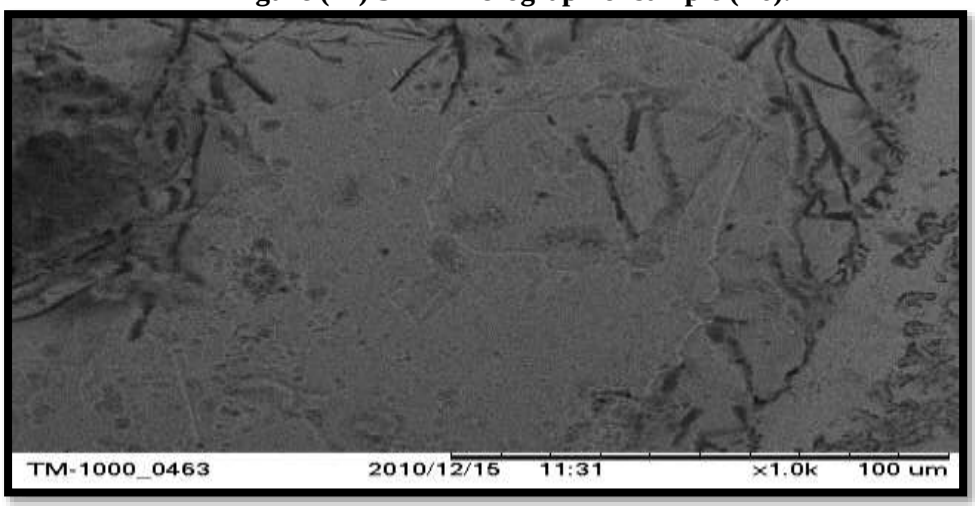

Figure (15) SEM micrograph of sample (N1).

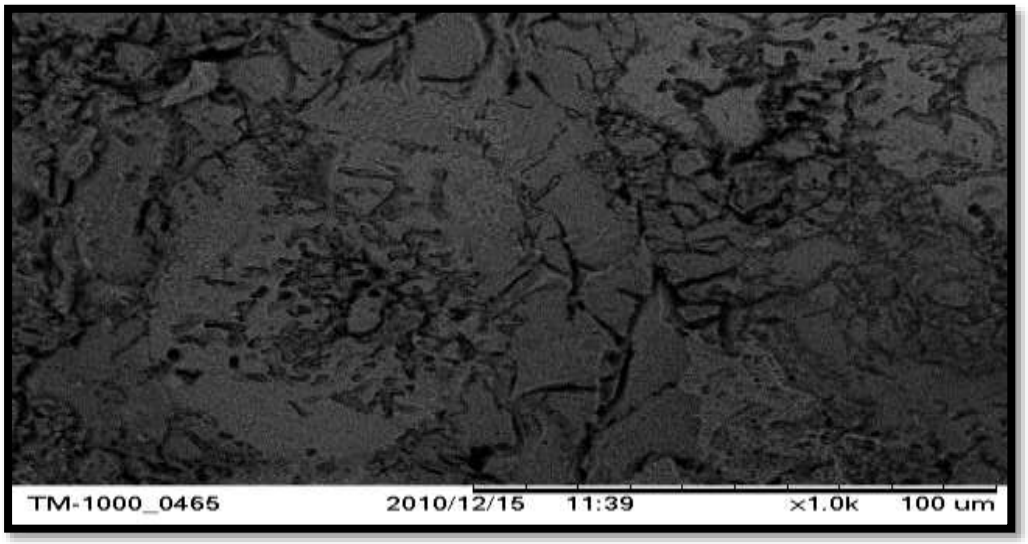

Figure (16) SEM micrograph of sample (N2).

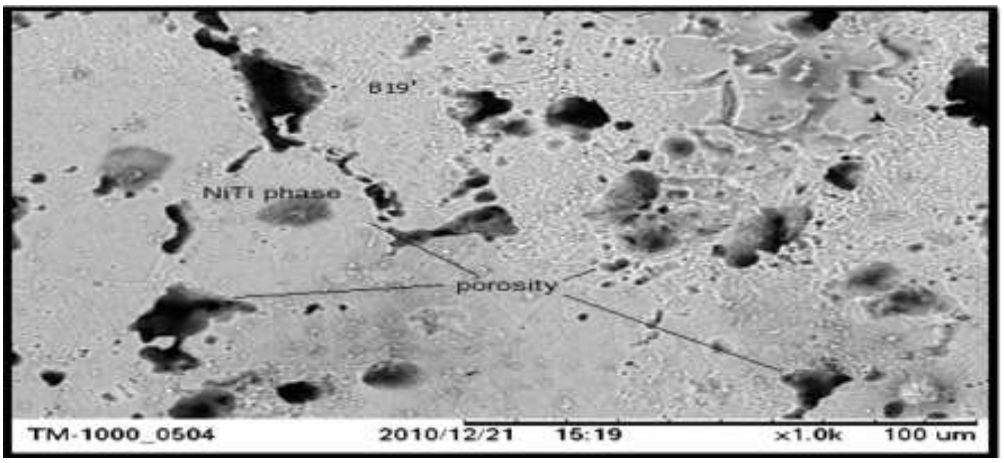

Figure (17) SEM micrograph of sample (N3).

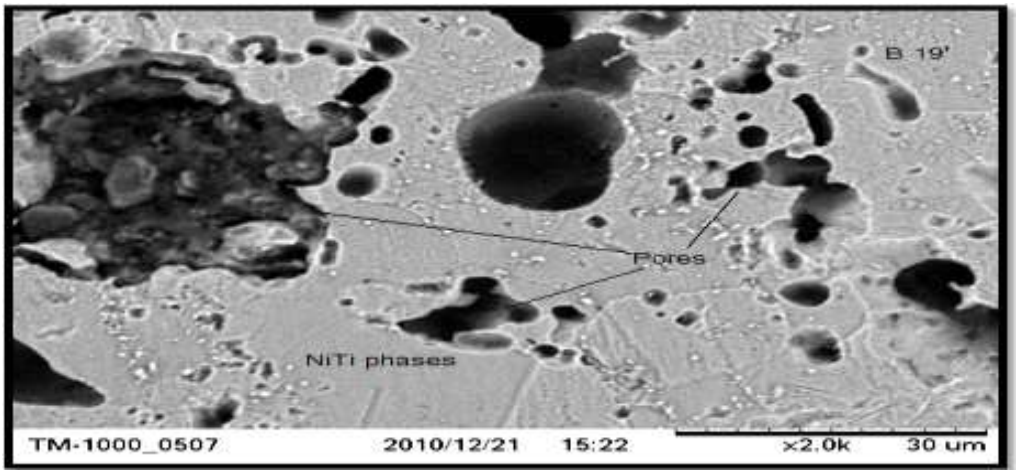

Figure (18) SEM micrograph of sample (N4).

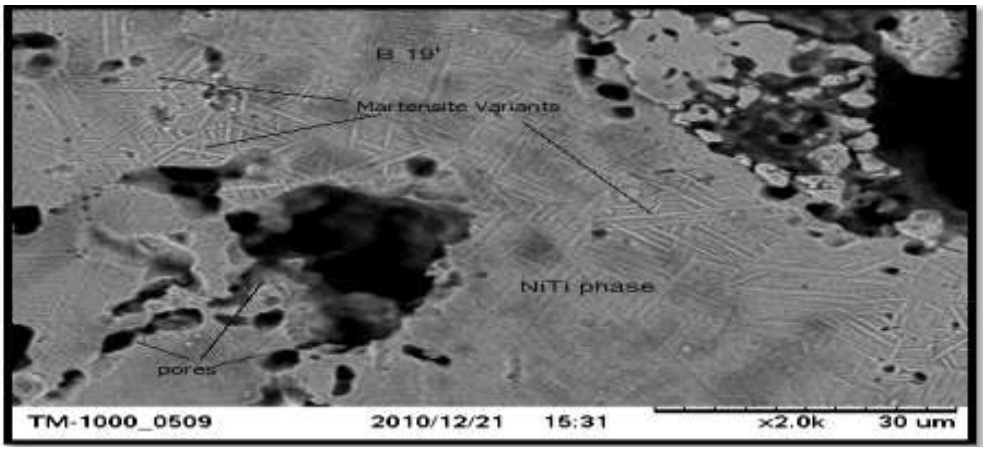

Figure (19) SEM micrograph of sample (N5).

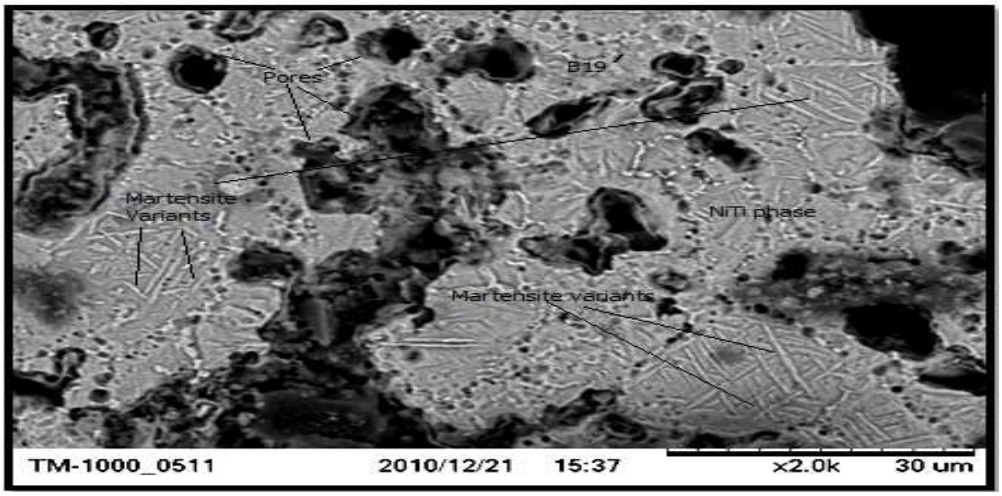

Figure (20) SEM micrograph of sample (N6).

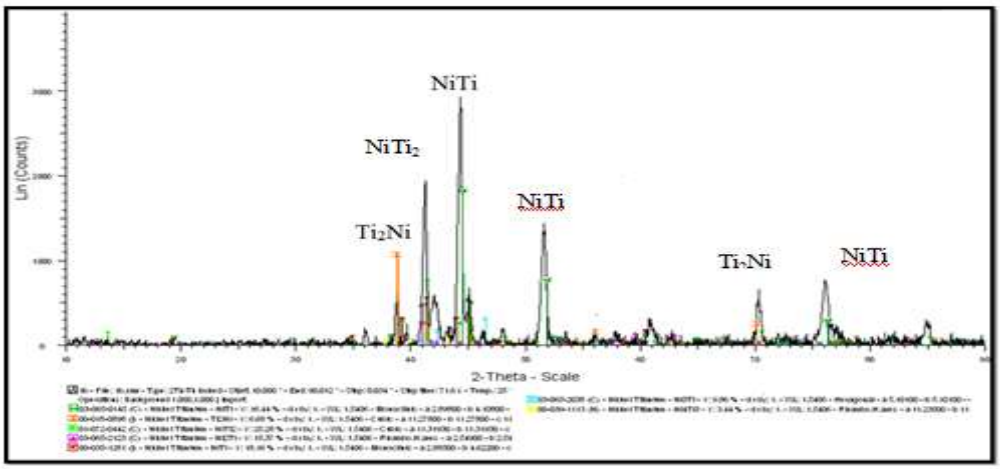

Figure (21) XRD pattern of sample (M1).

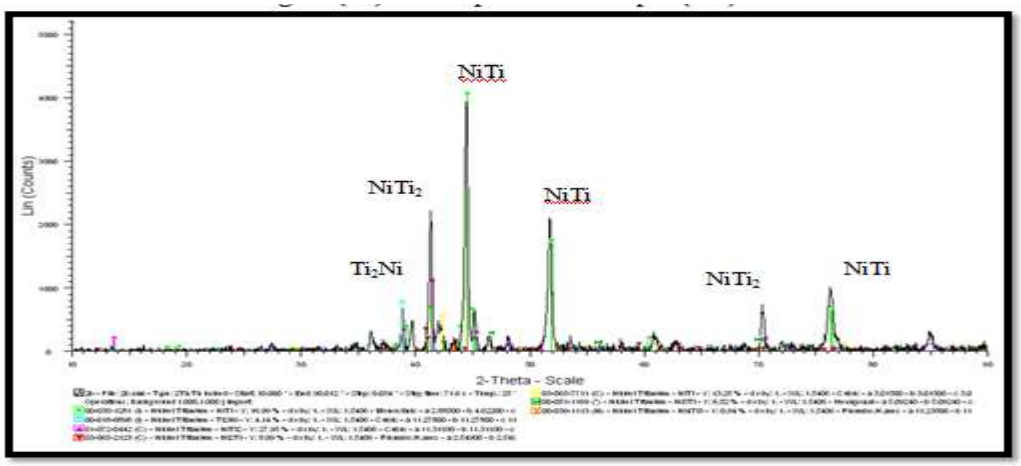

Figure (22) XRD pattern of sample (M2).

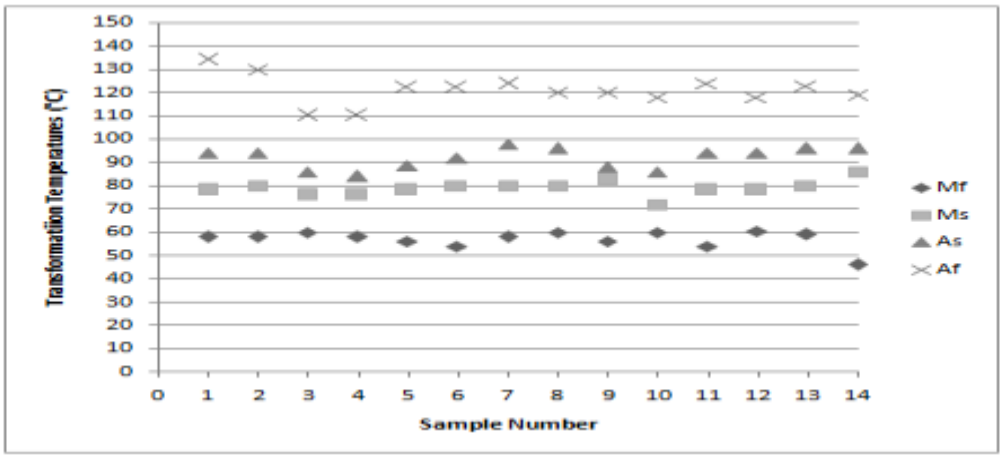

Figure (23) Transformation temperatures of austenitic and martensitic phases of all samples.

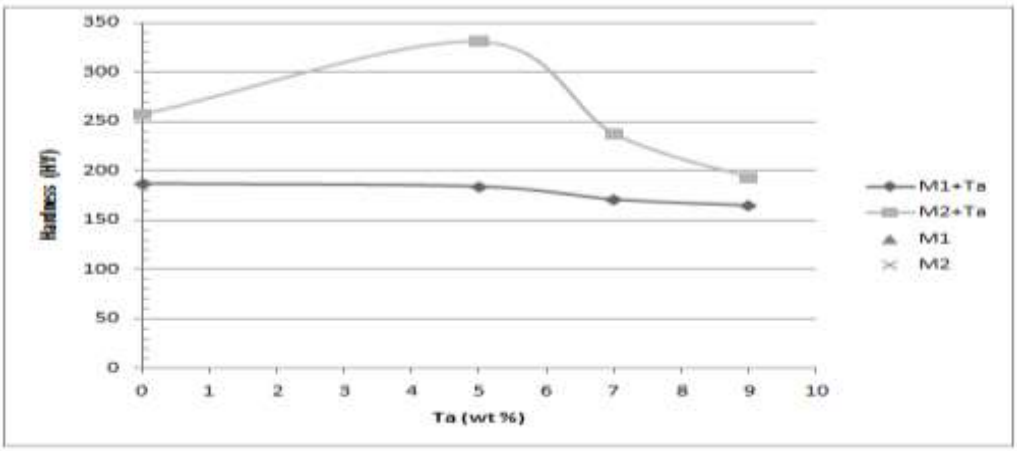

Figure (24) Hardness values for the master with various additives of Ta.

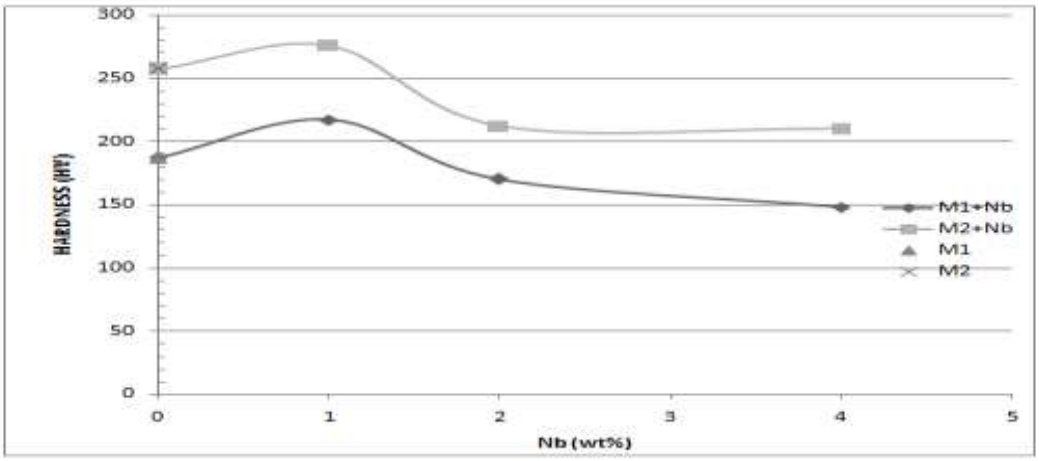

Figure (25) Hardness values for the master with various additives of Nb.

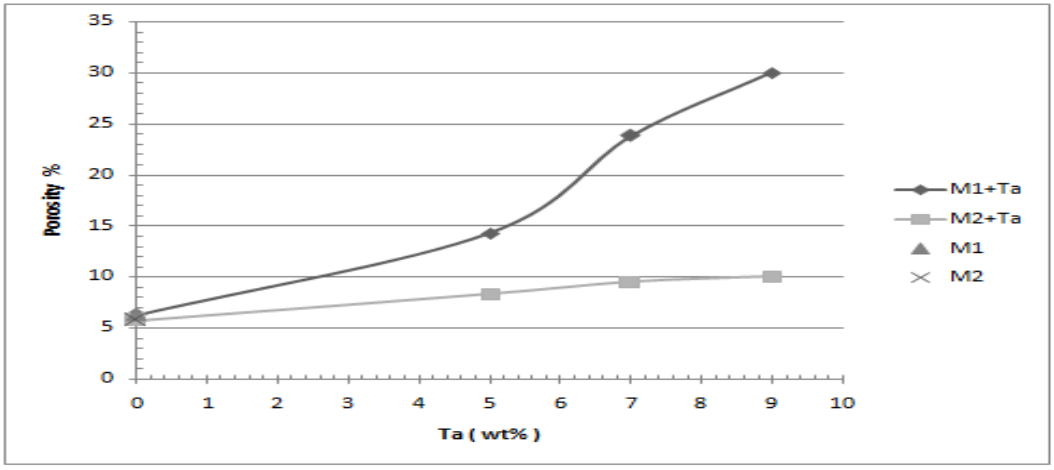

Figure (26) Porosity percentages for the master with various additives of Ta.

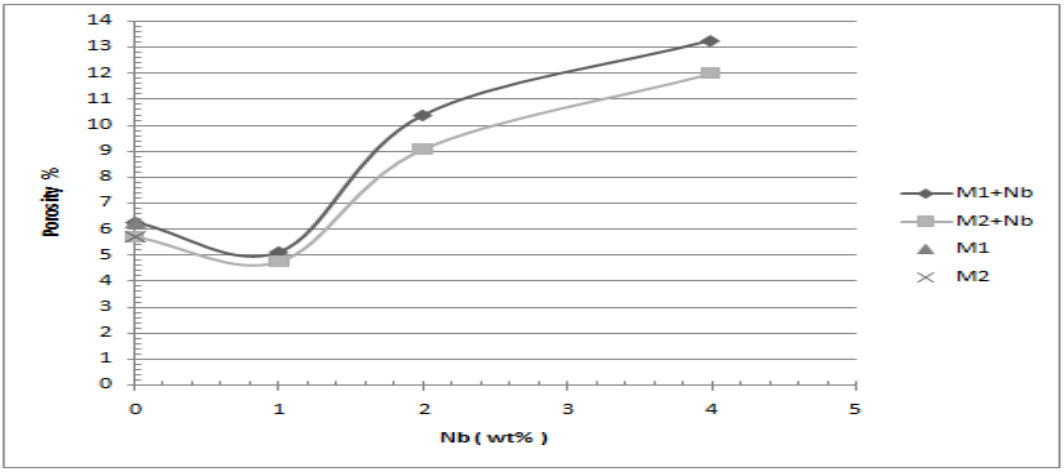

Figure (27) Porosity percentages for the master with various additives of Nb.